Inorganic Chemistry

pubs.acs.org/IC

Featured Article

Electron-Withdrawing *meso*-Substituents Turn On Magneto-Optical Activity in Porphyrins

Emigdio E. Turner, Trong-Nhan Pham, Samuel Peter Smith, Kaytlin N. Ward, Joel Rosenthal,* and Jeffrey J. Rack*

Cite This: *Inorg. Chem.* 2024, 63, 3630−3636

Read Online

ACCESS | Metrics & More | Article Recommendations | Supporting Information

ABSTRACT: A series of square planar metalloporphyrins (M(TPP), TPP is 5,10,15,20-tetraphenylporphyrin and M(TPFPP), TPFPP is 5,10,15,20-tetrapentafluorophenylporphyrin; M is Zn^{2+}, Ni^{2+}, Pd^{2+}, or Pt^{2+}) with distinct *meso*-substituents were prepared, and their magneto-optical activity (MOA) was characterized by magnetic circular dichroism (MCD) and magneto-optical rotary dispersion spectroscopy (MORD; also known as Faraday rotation spectroscopy). MOA is crucial in the development of next-generation magneto-optical devices and quantum computing. The data show that the presence of *meso*-pentafluorophenyl substituents results in significant increase in MOA in comparison to the homologous phenyl group. Differences in the MOA of these metalloporphyrins are rationalized using the Gouterman four-orbital model and pave the way for rational design of improved and tailorable magneto-optical materials.

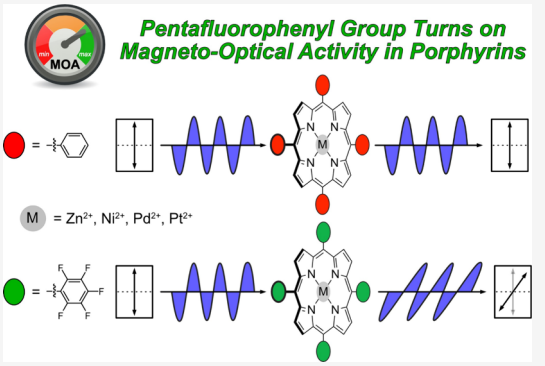

INTRODUCTION

Modern coherent optical light sources and photonic technologies are highly dependent on polarization modulators (e.g., Pockels cells). Polarization modulators or rotators are materials that allow left- and right-handed circularly polarized light to propagate at different speeds or phase velocities. Magneto-optical rotary dispersion (MORD) is the rotation of polarized light as it transmits through a magnetized material, also known as Faraday rotation (FR) or magnetic circular birefringence (MCB).[1] MORD and magnetic circular dichroism (MCD) are paired responses referred together as magneto-optical activity (MOA).[2−5] Current MOA components are typically fabricated from paramagnetic glasses and modulate polarization within changing magnetic fields.[6−8] The creation of molecular materials that exhibit MOA will open new applications and allow for the development of new technologies. Indeed, recent MOA reports highlight magnetic nanoparticles,[9−11] polymer thin films,[12−16] and other materials that show promise in this research space.[17−21]

MOA is characterized by Faraday A-, B-, and C-terms (eq 1) that are associated with a particular electronic transition from the ground state (G) to an excited state (J).[1,2,5] Briefly, Faraday A-terms (eq 1a) are operative when either a ground or excited electronic state is degenerate and Zeeman split in a magnetic field, where l_z is the angular momentum operator. Faraday B-terms (eq 1b) are manifest from magnetic field induced mixing of a third state (J') with either the ground or excited state of an electronic transition, where e is the charge on the electron and x and y are the polarized transition moment dipoles. Faraday B-terms are the weakest of the three terms and exist for all diamagnetic samples. This is the term responsible for the MOA in recently reported P3HT based polymers.[22−25] Zeeman split degenerate ground states yield C-terms (eq 1c), which are a consequence of unequal Boltzmann populations in each state at a given temperature. C-terms are predominantly exhibited by paramagnetic samples. These terms can be derived from MCD spectra using eqs 2 and 3. Eq 2 yields the dipole strength (D_0) of an electronic transition from $G \rightarrow J$ by fitting absorbance spectra in molar extinction units with a normalized Gaussian function (f). Eq 3 fits the change in extinction at a particular energy (E) in the absorption spectrum as a function of A, B, C terms, the Gaussian fit to the band (f) and magnetic field (H). In aggregate, these equations allow for evaluation of the rotation of light propagating through a material in a magnetic field. The rotation of light is due to differential speeds of left- and right-hand circularly polarized light as it passes through the medium.

$$A(G \rightarrow J) = \langle Jl|l_Z|J\rangle D_0(G \rightarrow J) \quad (1a)$$

Received: November 13, 2023
Revised: January 18, 2024
Accepted: January 23, 2024
Published: February 15, 2024

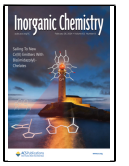

https://doi.org/10.1021/acs.inorgchem.3c04004
Inorg. Chem. 2024, 63, 3630−3636

$$B(G \rightarrow J) = \frac{\langle J|l_z|J'\rangle\langle G|-ex|J_x\rangle\langle J'_y|-ey|G\rangle}{3(E(J') - E(J))} \quad (1b)$$

$$C(G \rightarrow J) = \langle G|l_Z|G\rangle \mathrm{Im}(\langle G|-ex|J\rangle\langle J|-ey|G\rangle \quad (1c)$$

$$\epsilon/_E = 326.6 \times D_0(G \rightarrow J)f \quad (2)$$

$$\Delta\epsilon/_E = 152.5 \times H\left[A\left(-\frac{\partial f}{\partial E}\right) + \left(B + \frac{C}{kT}\right)f\right] \quad (3)$$

Based on the brief descriptions above, Faraday A-terms may be the most facile to engineer within materials as they simply require an intense electronic transition with a degenerate excited state, the latter of which is a direct consequence of molecular structure. The electronic structure and MCD spectra of highly symmetric metalloporphyrins have been well studied, but there are few papers describing their MORD activity,[26−32] or their use as magneto-optical polarization modulators.[15] The Gouterman four-orbital model simply describes the complicated electronic structure of porphyrins primarily through the interactions of two closely spaced (nearly degenerate) a_{1u} and a_{2u} HOMO orbitals and a degenerate e_g LUMO set.[33−36] Due to this degeneracy, we questioned if metalloporphyrins might be good candidates for next-generation polarization modulation materials. We hypothesized that e_g (d_{xz}, d_{yz}) metalporphyrin mixing (and introduction of charge transfer character) with the e_g LUMO would yield conditions favorable for excited state angular momentum transfer (eq 1a) thereby enhancing MOA through a Faraday A-term contribution. Herein, we report that simple square planar metalloporphyrins comprising electron-withdrawing *meso*-C_6F_5 substituents are enhanced Faraday rotators.[37] We provide an explanation for the observed increase in MOA of these porphyrins that invokes the Gouterman four-orbital model.

RESULTS AND DISCUSSION

Depicted in Chart 1 are the eight metalloporphyrins featured in this study. The two different porphyrins, 5,10,15,20-tetraphenylporphyrin (TPP, left) and 5,10,15,20-tetrapentafluorophenylporphyrin (TPFPP, right) were chosen to investigate the role of electron-withdrawing groups on MOA. This synthetic modification changes electron density on the porphyrin ring (a_{2u} HOMO; e_g LUMO) without changing the symmetry characteristics of the resulting molecular orbitals. The metal ions Zn^{2+}, Ni^{2+}, Pd^{2+}, and Pt^{2+} were chosen to address the role of metal size and extent of π-backbonding, with Zn^{2+} (d^{10}) being unable to participate in this interaction, due to the inaccessibility of Zn^{3+}. Alternatively, one may ascribe the lack of π-backbonding to the inaccessibility of the Zn^{2+} d-orbitals. As will be demonstrated below, a trend is seen across the M(TPFPP) compounds in which with increasing period of the group 10 metal (Ni^{2+}, Pd^{2+}, Pt^{2+}), enhancements of the MOA of the Q_0 transition are observed. This trend is reversed for the homologous TPP derivatives, indicating that the electron-withdrawing effects of the porphyrin *meso*-substituents plays a profound role in modulating the MOA response.

Chart 1. Molecular Structures of the Eight Metalloporphyrins Utilized in This Study

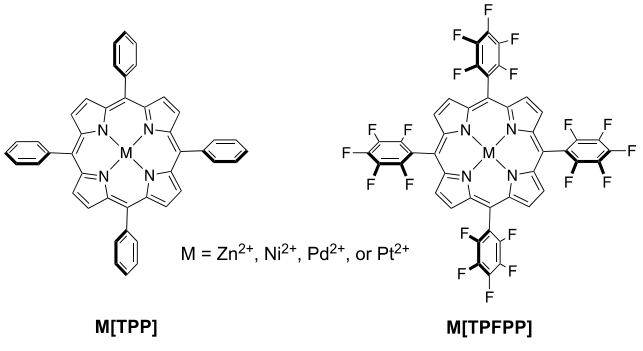

Shown in Figure 1A (top) are the absorbance spectra of **Zn(TPFPP)** (black), **Ni(TPFPP)** (red), **Pd(TPFPP)** (blue), and **Pt(TPFPP)** (green). An inset depicts an expanded spectral region containing the Q-bands. The peaks of each band, and their corresponding MOA terms and dipole strengths are summarized in Table 1. The Soret and Q-bands of the four TPFPP complexes shift to the blue with increasing period of the metal. The hypsochromic shift of the Ni^{2+}, Pd^{2+}, and Pt^{2+} porphyrins relative to the Zn^{2+} analogue is expected and has traditionally been ascribed to a metal d_{xz}, d_{yz} (e_g) bonding interaction with the $e_{g,x}$, $e_{g,y}$ LUMO orbital set.[33,34] Ghosh and Conradie have recently stated that the hypsochromic shift in the Soret is due to lowering of the a_{2u} HOMO (due to stabilization of the N 1s orbital) in their calculations of M(TPP) complexes, where M is Zn^{2+}, Pd^{2+}, and Pt^{2+}.[38] In addition, we note that the intensity (dipole strength) of the Soret band for the Ni^{2+}, Pd^{2+}, and Pt^{2+} is much weaker in comparison to the Zn^{2+} complex, suggesting that these metals affect the orbital contributions to the electronic transition.

The middle panel of Figure 1A depicts the measured MCD spectra of the four fluorinated metalloporphyrins. Focusing on the Soret band, one expects the MCD response to shift blue and to be weaker in intensity in accordance with the trends observed in the absorption spectra (top panel). Moreover, Faraday A-terms appear as first derivative line-shapes. Small asymmetries in the first derivative line-shapes to the blue of the Soret band are due to MCD B-terms. While the MCD response of the Q_0 band shifts blue (as expected from the absorbance spectra), there is a noticeable increase in the MCD response as a function of the size of the central metal ion.

For the group 10 series of metals, the intensity of the MCD band of Q_0 is largest for Pt^{2+} and smallest for Ni^{2+}. The Zn^{2+} complex features the lowest overall MCD intensity of the M(TPFPP) series, presumably due to its inability to engage in π-bonding with the porphyrin (Table 1). We will return to this point in our analysis of comparison with the M(TPP) systems (*vide infra*). These effects have been previously documented in porphyrins through their MCD spectra.[39−42]

The MORD spectra were estimated by calculating the Hilbert transform of the MCD response of each compound. Briefly, the Hilbert transform is an integral transform (Equation S2), which relates the real component (MORD) to the imaginary component (MCD) of the complex magnetically perturbed dielectric function. Practically, one computes the overlap of the MCD spectrum with a variable asymptotic function. The results of this analysis are shown in the bottom panels of Figure 1; this approach was first established by Stephens, and is much more straightforward than directly collecting the MORD (Faraday Rotation) spectrum.[5] Magneto-Optic A-terms appear as second derivative Gaussian lineshapes in the MORD spectra. The trends in

https://doi.org/10.1021/acs.inorgchem.3c04004
Inorg. Chem. 2024, 63, 3630−3636

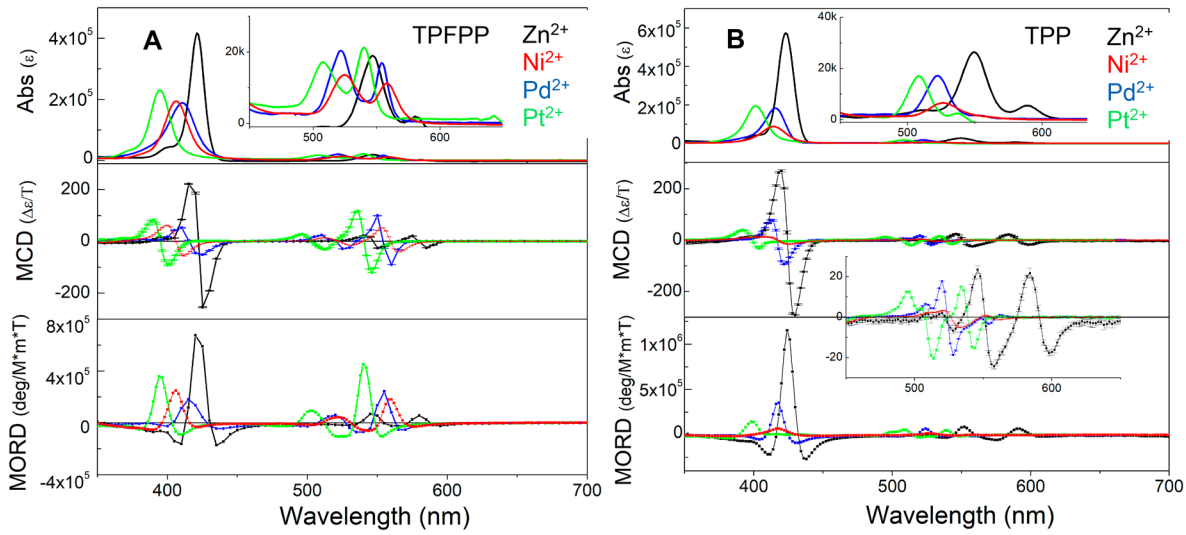

Figure 1. Absorbance (top), MCD (middle), and calculated MORD (bottom) spectra for A) **Zn(TPFPP)** (black), **Ni(TPFPP)** (red), **Pd(TPFPP)** (blue), and **Pt(TPFPP)** (green); and B) **Zn(TPP)** (black), **Ni(TPP)** (red), **Pd(TPP)** (blue), and **Pt(TPP)** (green).

Table 1. Absorption Maxima, MCD Terms, and Figure of Merit (FOM) for [M(TPP)] and M(TPFPP)], M = Zn^{2+}, Ni^{2+}, Pd^{2+}, Pt^{2+}

		M(TPP)[a]					M(TPFPP)[a]				
		λ_{max} (nm)	D_0	A	A/D_0	FOM	λ_{max} (nm)	D_0	A	A/D_0	FOM
Zn^{2+}	Q_0	589	0.53	1.36	2.57	0.12	580	0.52	0.92	1.77	0.30
	Q_1	550	3.55	1.70	0.48	0.03	547	3.11	1.34	0.43	0.04
	B_0[a]	423	56.4	31.6	0.56	0.02	421	33.9	25.0	0.74	0.02
Ni^{2+}	Q_0	565	0.10	0.07	0.7	0.02	559	1.12	3.30	2.95	0.16
	Q_1	527	1.26	0.59	0.47	0.03	525	2.39	1.87	0.78	0.03
	B_0	414	10.1	6.31	0.62	0.01	406	24.2	9.61	0.39	0.01
Pd^{2+}	Q_0	555	0.21	–	–	0.07	554	1.24	3.60	2.90	0.15
	Q_1	522	2.32	0.66	0.28	0.04	522	2.87	2.65	0.92	0.03
	B_0	416	19.5	9.93	0.51	0.02	411	24.6	12.6	0.51	0.01
Pt^{2+}	Q_0	537	0.36	0.48	1.33	0.21	540	1.62	6.22	3.84	0.21
	Q_1	508	2.49	0.29	0.12	0.03	508	2.18	3.28	1.50	0.07
	B_0	401	21.7	3.40	0.16	0.01	394	21.3	14.2	0.67	0.02

[a]For **Zn(TPP)** we use ε = 538,300 M^{-1} cm^{-1} at 424 nm, which is consistent with literature values and similar to the average value (560,000 M^{-1} cm^{-1}) recently suggested for use by Taniguchi, Lindsey, Bocian, and Holten.[43] For **Zn(TPFPP)**, we use ε = 5175 M^{-1} cm^{-1} at 589 nm (Q_0 peak max), which agrees well with Djerassi's original report (5050 M^{-1} cm^{-1} at 581 nm).[44]

the magnitude of relative MOA observed in the MCD spectra of the four M(TPFPP) complexes are preserved in the MORD spectra. Chiefly, there is an increase in the MOA of the Q_0 band. The MORD response of the Soret band definitively shows that these peaks shift blue relative to Zn^{2+}. Importantly, derived magneto-optic terms from either measurement (MCD or MORD), yield the same values for the dipole strength and Faraday terms (see Table 1).

Figure 1B contains the absorbance (top), MCD (middle), and calculated MORD (bottom) spectra for homologous metalloporphyrins bearing nonfluorinated phenyl substituents (i.e., **Zn(TPP)**, **Ni(TPP)**, **Pd(TPP)**, and **Pt(TPP)**), with relevant parameters shown in Table 1. The absorbance and MCD spectra we obtained are in good agreement with literature spectra.[43,45−47] Indeed, the absorbance spectra of the M(TPP) systems show an expected blue shift in their Soret maxima as the period of the metal increases, similar to what was observed for the fluorinated porphyrins. We note that for all four M(TPP) complexes, the Q_1 peak is more intense than the Q_0 peak, in contrast to what is observed for the M(TPFPP) homologues, where Q_0 and Q_1 peaks exhibit comparable intensity. Moreover, for **Pd(TPP)**, the Q_0 band is diminished to the point that its A-term contribution cannot be effectively calculated through fitting, as it appears as a shoulder on the red edge of the Q_1 band.

Strikingly, the trends seen for the increasing dipole strength (D_0) and MOA (A/D_0) in the Q_1 or Q_0 bands of the M(TPFPP) derivatives are not preserved for M(TPP). Instead, the MOA for the Q-bands *actually diminish* for **Pd(TPP)** and **Pt(TPP)** and is nearly nonexistent for **Ni(TPP)** as compared to that observed **for Zn(TPP)**. *Thus, for the TPP complexes, the d^8 metals quench angular momentum, while for the TPFPP samples, the metals enhance angular momentum and the formation of the magnetic dipole.* Our studies at this point do not provide an explanation for this reversal in activity, but it is a point of focus in our research at present.

Spectral features of porphyrins and metalloporphyrins are frequently rationalized using the Gouterman Four-Orbital model. The energy and intensity of the Soret band arises from the sum of electronic transition dipoles associated with the two

https://doi.org/10.1021/acs.inorgchem.3c04004
Inorg. Chem. 2024, 63, 3630−3636

one-electron transitions, $(a_{1u})^2(a_{2u})^1(e_{gx,y})^1$ and $(a_{1u})^1(a_{2u})^2(e_{gx,y})^1$, whereas the Q_0 band arises from their subtraction. The Q_1 band is a vibronic transition. In this series of complexes, the a_{1u} orbital is essentially constant as only the a_{2u} orbital features atomic contributions from the *meso*-carbon atoms (the electronics of which are perturbed by attachment to either C_6H_5 or C_6F_5 groups). Djerassi has argued that the a_{2u} orbital is actually lower in energy than the a_{1u} orbital in **Zn(TPFPP)**, whereas this ordering is reversed in **Zn(TPP)**.[44,48] However, recent calculations on **Pd(TPFPP)** show the a_{2u} to be of higher energy than the a_{1u} orbital.[49] Nevertheless, the precise ordering of these orbitals and their energy difference will be determined by a complicated mix of interactions involving the *meso*- substituent, metal based orbitals and the a_{2u} orbital.

We have found no literature report comprising computational results for all the complexes included in this study. Thus, DFT calculations were performed to gain insight into the electronic structure for each of the eight metalloporphyrins detailed herein. Shown in Figure 2 are the molecular orbital

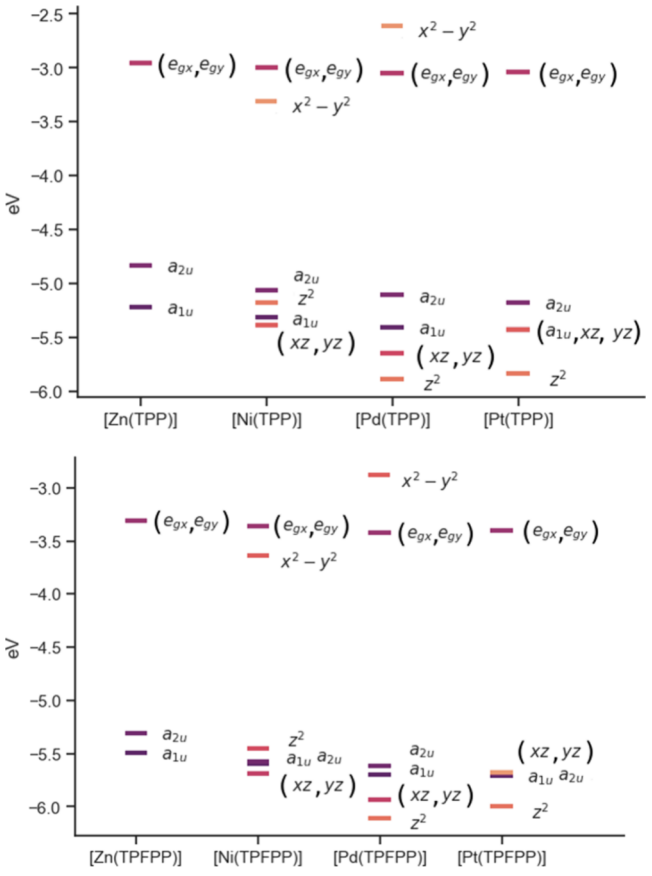

Figure 2. Molecular orbital energy diagrams for M(TPP) and M(TPFPP) complexes, where M = Zn^{2+}, Ni^{2+}, Pd^{2+}, Pt^{2+}.

diagrams for each metalloporphyrin. These data reveal the following trends. (1) In all cases, the a_{2u} orbital is higher in energy than the a_{1u} orbital, and the energy of the a_{1u} is largely invariant for both sets of complexes (Figure 2; Table S1). (2) As expected, the a_{1u} energies are lower for the M(TPFPP) complexes relative to the M(TPP) homologues. (3) The presence of the group 10 metals (Ni, Pd, Pt) appear to stabilize (lower) the energy of both the a_{1u} and a_{2u} orbitals relative to both Zn(TPP) and Zn(TPFPP).

Importantly, we note that the $a_{1u} - a_{2u}$ energy gap (Table S1) is distinctly larger for all of the M(TPP) complexes (Zn^{2+}: −0.39 eV; Ni^{2+}: −0.25 eV; Pd^{2+}: −0.30 eV; Pt^{2+}: −0.26 eV) as compared to that for the M(TPFPP) systems (Zn^{2+}: −0.18 eV; Ni^{2+}: −0.02 eV; Pd^{2+}: −0.07 eV; Pt^{2+}: −0.03 eV). This point is considered in greater detail below. We also observe that the group 10 metal based d_{xz}, and d_{yz} orbitals are close in energy to the a_{1u} and a_{2u} pair. Consistent with literature reports, the LUMO is the porphyrin-localized e_g orbital set for each of the metalloporphryins we have considered except the Ni^{2+} complexes, which show the d_{x2-y2} orbital to be very close in energy to the e_g orbital set. Lastly, the *d*-orbital contribution (determined from Mulliken analysis) to the e_g orbital set is small across the series ranging from 2 to 4% (Table S2). Moreover, when comparing any M(TPP) derivative to its M(TPFPP) homologue (e.g., Ni(TPP) vs N(TPFPP), etc.), we find the *d*-orbital contributions are almost identical, suggesting that a change in π-backbonding from the metal may not be responsible for the increase in MOA observed for the M(TPFPP) systems.

Table 1 summarizes the spectral characteristics observed for the M(TPP) and M(TPFPP) systems. To account for differences in intensity of the electronic transition (ε), we compare A/D_0 values, which allows for a direct comparison of MOA for a specific band within a set of compounds. A more intense electronic transition will necessarily feature greater MOA. For the M(TPP) derivatives, we calculated A/D values of 0.56 (Zn), 0.62 (Ni), 0.51 (Pd), and 0.16 (Pt) for the Soret (B) transition, which are in good agreement with the previously reported a value of 0.73 for Zn(TPP) by Ceulemans.[39] A similar trend is observed for the Q_1 peak as A/D values of 0.48 (Zn), 0.47 (Ni), 0.26 (Pd), and 0.12 (Pt) were calculated, indicating a loss of magneto-optical activity with increasing period of the metal.

The above results are surprising since one might anticipate an increase in metal−ligand orbital mixing with the inclusion of Ni^{2+}, Pd^{2+}, or Pt^{2+} in place of Zn^{2+}, the latter of which cannot engage in π-backbonding. In contrast to the M(TPP) derivatives, calculated A/D_0 values for both Q_0 and Q_1 peaks within the M(TPFPP) series show a substantial increase in MOA for the Q_0 and Q_1 peaks from Zn (1.77; 0.43, respectively) to Ni (2.95; 0.78) to Pd (2.89; 0.92) to Pt (3.84; 1.5). Indeed, there is a considerable increase in the MOA of **Pd(TPFPP)** and **Pt(TPFPP)** as compared to their M(TPP) homologues. It is perhaps not surprising that the Soret band shows little MOA activity. While the electronic dipoles for the Soret transition are additive, their magnetic dipoles are subtractive. The inverse relationship holds for Q bands, thus providing a justification as to why the Q-bands exhibit greater MOA than the Soret band.

Which factor or factors explain this dramatic change in MOA between the fluorinated and nonfluorinated porphyrins? eq 1a shows that the Faraday A-term is a direct measure of the angular momentum transfer between the $e_{g,x}$ and $e_{g,y}$ orbitals ($\langle J_x | l_z | J_y \rangle$) forming the LUMO set. *In other words, it is a measure of the magnitude of the magnetic dipole formed in the excited state following the electronic transition.* One proposal to explain the increase in MOA for the M(TPFPP) complexes is an increase in metal character in the e_g orbital set. However, as noted previously, the amount of *d*-orbital character for M(TPP) and M(TPFPP) is rather low, suggesting that this is not likely the origin of the increased MOA.

https://doi.org/10.1021/acs.inorgchem.3c04004
Inorg. Chem. 2024, 63, 3630−3636

Consideration of the Gouterman four orbital model leads to another potential explanation of the MOA trends. Configuration interaction occurs when the $a_{1u}a_{2u}$ HOMO orbital set ceases to be degenerate, resulting in mixing of the B band with the Q bands. The mixing parameter (ν) scales as the $a_{1u} - a_{2u}$ energy gap by the relation,

$$\tan 2\nu = \frac{(Ea_{1u} - Ea_{2u})}{2(E_B - E_Q)} \quad (4)$$

where E_{a1u}, E_{a2u} are the orbital energies of the a_{1u} and a_{2u} orbitals, respectively, and E_B and E_Q are the observed energy maxima (in cm^{-1}) of the B (Soret) and Q_0 electronic transitions, respectivly.[39] Thus, ν and mixing is reduced when the a_{1u}, a_{2u} orbital set is degenerate or nearly so. As the Soret transition involves subtraction of magnetic dipoles, integration of this transition within the Q-band, where magnetic dipoles are added, would appear to reduce MOA. By this reasoning, porphyrins with large a_{1u}, a_{2u} energy gaps should exhibit reduced MOA relative to porphyrins with smaller HOMO energy gaps, as found in the series we present here. We are currently pursuing this design strategy in order to maximize MOA in porphyrins and other tetrapyrrole platforms.[50−59]

Recent studies of magneto-optical materials for polarization control have often been characterized by two different figures of merit (FOM).[60] The Verdet constant has been used for over a century to describe the rotary power of FR (Faraday Rotation; MORD) materials at a specific wavelength. It is evaluated from the relation

$$\theta = VBL \quad (5)$$

where the degree of rotation (Θ) is determined by the Verdet constant (V), the magnetic field (B) and the thickness of the sample (L). It does not account for regions of absorbance and presumes the material under study is completely transparent. It does not account for the intrinsic absorptivity of the sample. This parameter is particularly advantageous when determining MOA for thin films, where accurate and precise values of extinction can very often be difficult to obtain.

A second FOM recently introduced by Swager characterizes FR in regions of absorbance.[61,62] This FOM is simply FR (MORD) at a particular wavelength (often a peak absorbance maximum) divided by the applied field and absorbance at that wavelength. This FOM is designed to evaluate a material's ability to rotate polarization at a selected wavelength and is not formulated to convey specific molecular information. Unlike the Verdet constant, it is not dependent on the thickness of a sample and can be readily calculated for molecules in solution.

Using Swager's approach, we have calculated the FOM for these square planar metalloporphyrins at the peak of the MORD spectra (see Table 1). Many of the FOM values reported here are an order of magnitude larger than those reported earlier for related porphyrin and phthalocyanine compounds ($\sim 10^{-2}$).[15] However, the calculated FOM values do not follow the trends observed in MCD and MORD spectra of the metalloporphyrins that we have studied. For example, the highest FOM is associated with the Q_0 band of Zn(TPFPP), which has the lowest MOA out of the four M(TPFPP) systems presented here. One explanation for this is that the FOM only selects a single wavelength and does not account for the entire band line shape (f) or intensity (dipole strength, D_0) of the transition. While the FOM is ideal for evaluating MOA of a particular material at a specific wavelength, it does not fully account for the origin of MOA.

CONCLUSION

Designing small molecules with large MOA for polarization control requires an understanding of the electronic structural elements that yield MOA.[60] This study illustrates that metalloporphyrins containing strongly electron-withdrawing C_6F_5 groups at the *meso*-positions lead to a significant increase in MOA when compared to their nonfluorinated homologues. The observed MOA in each metalloporphyrin is rationalized through the Gouterman four orbital model. Further work is underway to uncover the precise role of metalloporphyrin *meso*-substituents in affecting the HOMO energy gap and the resulting MOA of such derivatives. These results will compel future studies involving tetrapyrrole materials that can form the basis of next-generation magneto-optical polarization modulators.

ASSOCIATED CONTENT

Supporting Information

The Supporting Information is available free of charge at https://pubs.acs.org/doi/10.1021/acs.inorgchem.3c04004.

Experimental procedures, synthetic details, a complete description of the instrument, DFT calculations, and our analytical procedure for fitting data and extracting Faraday terms (PDF)

AUTHOR INFORMATION

Corresponding Authors

Jeffrey J. Rack − *Department of Chemistry and Chemical Biology, Laboratory for Magneto-Optic Spectroscopy, University of New Mexico, Albuquerque, New Mexico 87131, United States;* orcid.org/0000-0001-6121-879X; Email: jrack@unm.edu

Joel Rosenthal − *Department of Chemistry and Biochemistry, University of Delaware, Newark, Delaware 19711, United States;* orcid.org/0000-0002-6814-6503; Email: joelr@udel.edu

Authors

Emigdio E. Turner − *Department of Chemistry and Chemical Biology, Laboratory for Magneto-Optic Spectroscopy, University of New Mexico, Albuquerque, New Mexico 87131, United States*

Trong-Nhan Pham − *Department of Chemistry and Biochemistry, University of Delaware, Newark, Delaware 19711, United States;* orcid.org/0000-0002-5087-0421

Samuel Peter Smith − *Department of Chemistry and Chemical Biology, Laboratory for Magneto-Optic Spectroscopy, University of New Mexico, Albuquerque, New Mexico 87131, United States;* orcid.org/0009-0000-5612-5804

Kaytlin N. Ward − *Department of Chemistry and Biochemistry, University of Delaware, Newark, Delaware 19711, United States;* orcid.org/0000-0002-3141-0454

Complete contact information is available at: https://pubs.acs.org/10.1021/acs.inorgchem.3c04004

Notes

The authors declare no competing financial interest.

https://doi.org/10.1021/acs.inorgchem.3c04004
Inorg. Chem. 2024, 63, 3630−3636

■ ACKNOWLEDGMENTS

This work was supported by NSF CHE 1856492 (J.J.R., UNM), 2247761 (J.J.R., UNM), and through the U.S. Department of Energy, Office of Science, Office of Basic Energy Sciences EPSCoR and Catalysis programs under Award Number DESC-0001234 (J.R., UD). Research reported in this publication was also supported by the National Institute of General Medical Sciences of the National Institutes of Health under Award Number T32GM133395. The content is solely the responsibility of the authors and does not necessarily represent the official views of the National Institutes of Health. We thank the UNM Center for Advanced Research Computing supported in part by the National Science Foundation for providing the high-performance computing resources used this work.

■ REFERENCES

(1) Barron, L. *Molecular Light Scattering and Optical Activity*; Cambridge University Press, 2004.
(2) Buckingham, A. D.; Stephens, P. J. Magnetic Optical Activity. *Annu. Rev. Phys. Chem.* **1966**, *17*, 399.
(3) Stephens, P. J. Excited state magnetic moments through moment analysis of magnetic circular dichroism. *Chem. Phys. Lett.* **1968**, *2* (4), 241−244.
(4) Stephens, P. J. Theory of Magnetic Circular Dichroism. *J. Chem. Phys.* **1970**, *52* (7), 3489.
(5) Stephens, P. J. Magnetic Circular-Dichroism. *Annu. Rev. Phys. Chem.* **1974**, *25*, 201−232.
(6) Barnes, N. P.; Petway, L. B. Variation of the Verdet Constant with Temperature of Terbium Gallium Garnet. *J. Opt. Soc. Am. B* **1992**, *9* (10), 1912−1915.
(7) Yasuhara, R.; Tokita, S.; Kawanaka, J.; Kawashima, T.; Kan, H.; Yagi, H.; Nozawa, H.; Yanagitani, T.; Fujimoto, Y.; Yoshida, H.; et al. Cryogenic temperature characteristics of Verdet constant on terbium gallium garnet ceramics. *Opt. Express* **2007**, *15* (18), 11255−11261.
(8) Yoshida, H.; Tsubakimoto, K.; Fujimoto, Y.; Mikami, K.; Fujita, H.; Miyanaga, N.; Nozawa, H.; Yagi, H.; Yanagitani, T.; Nagata, Y.; et al. Optical properties and Faraday effect of ceramic terbium gallium garnet for a room temperature Faraday rotator. *Opt. Express* **2011**, *19* (16), 15181−15187.
(9) Han, B.; Gao, X.; Lv, J.; Tang, Z. Magnetic Circular Dichroism in Nanomaterials: New Opportunity in Understanding and Modulation of Excitonic and Plasmonic Resonances. *Adv. Mater.* **2020**, *32* (41), 1801491.
(10) Liu, X.; Du, Y.; Mourdikoudis, S.; Zheng, G.; Wong, K.-Y. Chiral Magnetic Oxide Nanomaterials: Magnetism Meets Chirality. *Advanced Optical Materials* **2023**, DOI: 10.1002/adom.202202859.
(11) Carothers, K. J.; Lyons, N. P.; Pavlopoulos, N. G.; Kang, K.-S.; Kochenderfer, T. M.; Phan, A.; Holmen, L. N.; Jenkins, S. L.; Shim, I.-B.; Norwood, R. A.; et al. Polymer-Coated Magnetic Nanoparticles as Ultrahigh Verdet Constant Materials: Correlation of Nanoparticle Size with Magnetic and Magneto-Optical Properties. *Chem. Mater.* **2021**, *33* (13), 5010−5020.
(12) Araoka, F.; Abe, M.; Yamamoto, T.; Takezoe, H. Large Faraday Rotation in a pi-Conjugated Poly(arylene ethynylene) Thin Film. *Applied Physics Express* **2009**, *2* (1), 011501.
(13) Dall'Agnol, F. F.; Shimizu, F. M.; Giacometti, J. A. Determination of photoinduced and intrinsic birefringences in PMMA/DR13 guest-host film. *Chem. Phys. Lett.* **2014**, *608*, 102−105.
(14) Liu, X.; Turner, E. E.; Sharapov, V.; Yuan, D.; Awais, M. A.; Rack, J. J.; Yu, L. Finely Designed P3HT-Based Fully Conjugated Graft Polymer: Optical Measurements, Morphology, and the Faraday Effect. *ACS Appl. Mater. Interfaces* **2020**, *12* (27), 30856−30861.
(15) Nelson, Z.; Delage-Laurin, L.; Peeks, M. D.; Swager, T. M. Large Faraday Rotation in Optical-Quality Phthalocyanine and Porphyrin Thin Films. *J. Am. Chem. Soc.* **2021**, *143* (18), 7096−7103.
(16) Vleugels, R.; de Vega, L.; Brullot, W.; Verbiest, T.; Gomez-Lor, B.; Gutierrez-Puebla, E.; Hennrich, G. Magneto-optical activity in organic thin film materials. *Smart Materials and Structures* **2016**, *25* (12), 12LT01.
(17) Carothers, K. J.; Norwood, R. A.; Pyun, J. High Verdet Constant Materials for Magneto-Optical Faraday Rotation: A Review. *Chem. Mater.* **2022**, *34* (6), 2531−2544.
(18) Ikesue, A.; Aung, Y. L.; Wang, J. Progress of magneto-optical ceramics. *Progress in Quantum Electronics* **2022**, *86*, 100416.
(19) Srinivasan, K.; Stadler, B. J. H. Review of integrated magneto-optical isolators with rare-earth iron garnets for polarization diverse and magnet-free isolation in silicon photonics Invited. *Optical Materials Express* **2022**, *12* (2), 697−716.
(20) Zhang, L.; Hu, D.; Snetkov, I. L.; Balabanov, S.; Palashov, O.; Li, J. A review on magneto-optical ceramics for Faraday isolators. *Journal of Advanced Ceramics* **2023**, *12* (5), 873−915.
(21) Zhang, Z.; Wu, Z.; Zhang, Z.; Su, L.; Wu, A.; Li, Y.; Lan, J. Characteristics and Recent Development of Fluoride Magneto-Optical Crystals. *Magnetochemistry* **2023**, *9* (2), 41.
(22) Gangopadhyay, P.; Voorakaranam, R.; Lopez-Santiago, A.; Foerier, S.; Thomas, J.; Norwood, R. A.; Persoons, A.; Peyghambarian, N. Faraday rotation measurements on thin films of regioregular alkyl-substituted polythiophene derivatives. *J. Phys. Chem. C* **2008**, *112* (21), 8032−8037.
(23) Koeckelberghs, G.; Vangheluwe, M.; Van Doorsselaere, K.; Robijns, E.; Persoons, A.; Verbiest, T. Regioregularity in poly(3-alkoxythiophene)s: Effects on the Faraday rotation and polymerization mechanism. *Macromol. Rapid Commun.* **2006**, *27* (22), 1920−1925.
(24) Lopez-Santiago, A.; Gangopadhyay, P.; Thomas, J.; Norwood, R. A.; Persoons, A.; Peyghambarian, N. Faraday rotation in magnetite-polymethylmethacrylate core-shell nanocomposites with high optical quality. *Appl. Phys. Lett.* **2009**, *95* (14), 143302.
(25) Gangopadhyay, P.; Koeckelberghs, G.; Persoons, A. Magneto-optic Properties of Regioregular Polyalkylthiophenes. *Chem. Mater.* **2011**, *23* (3), 516−521.
(26) Birnbaum, T.; Hahn, T.; Martin, C.; Kortus, J.; Fronk, M.; Lungwitz, F.; Zahn, D. R. T.; Salvan, G. Optical and magneto-optical properties of metal phthalocyanine and metal porphyrin thin films. *J. Phys.: Condens. Matter* **2014**, *26* (10), 104201.
(27) Mulyana, Y.; Ishii, K. A novel aspect of spectroscopy for porphyrinic compounds under magnetic fields. *Dalton Transactions* **2014**, *43* (47), 17596−17605.
(28) Ristau, O.; Rein, H. Quantitative-Analysis of Absorption-Spectra and Spectra of Magneto-Optical Rotatory-Dispersion of Hemoproteins with Regard to Zero-Field Splitting.1. Analysis of Dication of Deuteroporphyrin in Q-Band Region. *Acta Biologica Et Medica Germanica* **1976**, *35* (12), 1613−1624.
(29) Sharonov, Y. A.; Sharonova, N. A.; Atanasov, B. P. Dependence of Magneto-Optical Rotatory-Dispersion and Magnetic Circular-Dichroism of Deoxyhemoglobin and Methemoglobin on Their Quaternary Structure. *Biochimica Et Biophysica Acta* **1976**, *434* (2), 440−451.
(30) Shashoua, V. E. Magneto-optical Rotation Spectra of Porphyrins and Phthalocyanines. *J. Am. Chem. Soc.* **1965**, *87* (18), 4044−4048.
(31) Shashoua, V. E. Magneto optical rotation spectroscopy. *Methods Enzymol.* **1973**, *27*, 796−810.
(32) Stephens, P. J.; Mowery, R. L.; Schatz, P. N. Moment Analysis of Magnetic Circular Dichroism: Diamagnetic Molecular Solutions. *J. Chem. Phys.* **1971**, *55* (1), 224−231.
(33) Gouterman, M. Study of the Effects of Substitution on the Absorption Spectra of Porphin. *J. Chem. Phys.* **1959**, *30* (5), 1139−1161.
(34) Gouterman, M. Spectra of porphyrins. *J. Mol. Spectrosc.* **1961**, *6* (1), 138−163.
(35) Gouterman, M.; Snyder, L. C.; Wagniere, G. H. SPECTRA OF PORPHYRINS.2. 4 ORBITAL MODEL. *J. Mol. Spectrosc.* **1963**, *11* (1-6), 108−127.

https://doi.org/10.1021/acs.inorgchem.3c04004
Inorg. Chem. 2024, 63, 3630−3636

(36) Weiss, C.; Kobayashi, H.; Gouterman, M. Spectra of porphyrins. *J. Mol. Spectrosc.* **1965**, *16* (2), 415−450.
(37) Turner, E. E.; Pham, T.-N.; Smith, S. P.; Ward, K.; Rosenthal, J.; Rack, J. J. Electron Withdrawing meso-Substituents Turn-on Magneto-Optical Activity in Porphyrins. *ChemRxiv* **2023**, DOI: 10.26434/chemrxiv-2023-7s018.
(38) Ghosh, A.; Conradie, J. The Dog That Didn't Bark: A New Interpretation of Hypsoporphyrin Spectra and the Question of Hypsocorroles. *J. Phys. Chem. A* **2021**, *125* (46), 9962−9968.
(39) Ceulemans, A.; Oldenhof, W.; Gorllerwalrand, C.; Vanquickenborne, L. G. Gouterman 4-Orbital Model and the Mcd Spectra of High-Symmetry Metalloporphyrins. *J. Am. Chem. Soc.* **1986**, *108* (6), 1155−1163.
(40) Mack, J.; Asano, Y.; Kobayashi, N.; Stillman, M. J. Application of MCD spectroscopy and TD-DFT to a highly non-planar porphyrinoid ring system. New insights on red-shifted porphyrinoid spectral bands. *J. Am. Chem. Soc.* **2005**, *127* (50), 17697−17711.
(41) Mack, J.; Stillman, M. J. Assignment of the optical spectra of metal phthalocyanines through spectral band deconvolution analysis and ZINDO calculations. *Coord. Chem. Rev.* **2001**, *219-221*, 993−1032.
(42) Mack, J.; Stillman, M. J.; Kobayashi, N. Application of MCD spectroscopy to porphyrinoids. *Coord. Chem. Rev.* **2007**, *251* (3−4), 429−453.
(43) Taniguchi, M.; Lindsey, J. S.; Bocian, D. F.; Holten, D. Comprehensive review of photophysical parameters (epsilon, Phi(f), tau(s)) of tetraphenylporphyrin (H2TPP) and zinc tetraphenylporphyrin (ZnTPP) - Critical benchmark molecules in photochemistry and photosynthesis. *Journal of Photochemistry and Photobiology C-Photochemistry Reviews* **2021**, *46*, 100401.
(44) Keegan, J. D.; Bunnenberg, E.; Djerassi, C. Magnetic Circular-Dichroism Studies.63. Sign Variation in the Magnetic Circular-Dichroism Spectra of Some Perimeter Symmetric Metallo Porphyrins. *Spectrochimica Acta Part a-Molecular and Biomolecular Spectroscopy* **1984**, *40* (3), 287−297.
(45) Che, C. M.; Hou, Y. J.; Chan, M. C. W.; Guo, J. H.; Liu, Y.; Wang, Y. meso-Tetrakis(pentafluorophenyl)porphyrinato platinum-(II) as an efficient, oxidation-resistant red phosphor: spectroscopic properties and applications in organic light-emitting diodes. *J. Mater. Chem.* **2003**, *13* (6), 1362−1366.
(46) To, W.-P.; Liu, Y.; Lau, T.-C.; Che, C.-M. A Robust Palladium(II)-Porphyrin Complex as Catalyst for Visible Light Induced Oxidative C-H Functionalization. *Chem.—Eur. J.* **2013**, *19* (18), 5654−5664.
(47) Hodge, J. A.; Hill, M. G.; Gray, H. B. Electrochemistry of Nonplanar Zinc(Ii) Tetrakis(Pentafluorophenyl)Porphyrins. *Inorg. Chem.* **1995**, *34* (4), 809−812.
(48) Keegan, J. D.; Bunnenberg, E.; Djerassi, C. Magnetic Circular-Dichroism Studies.62. Sign Variation in the Magnetic Circular-Dichroism Spectra of Some Perimeter Symmetric Free-Base Porphyrins. *Spectrosc. Lett.* **1983**, *16* (4), 275−286.
(49) Martin, S. M.; Repa, G. M.; Hamburger, R. C.; Pointer, C. A.; Ward, K.; Pham, T.-N.; Martin, M. I.; Rosenthal, J.; Fredin, L. A.; Young, E. R. Elucidation of complex triplet excited state dynamics in Pd(ii) biladiene tetrapyrroles. *Phys. Chem. Chem. Phys.* **2023**, *25* (3), 2179−2189.
(50) Cai, Q.; Rice, A. T.; Pointer, C. A.; Martin, M. I.; Davies, B.; Yu, A.; Ward, K.; Hertler, P. R.; Warndorf, M. C.; Yap, G. P. A.; et al. Synthesis, Electrochemistry, and Photophysics of Pd(II) Biladiene Complexes Bearing Varied Substituents at the sp(3)-Hybridized 10-Position. *Inorg. Chem.* **2021**, *60* (20), 15797−15807.
(51) Cai, Q.; Tran, L. K.; Qiu, T.; Eddy, J. W.; Trong-Nhan, P.; Yap, G. P. A.; Rosenthal, J. An Easily Prepared Monomeric Cobalt(II) Tetrapyrrole Complex That Efficiently Promotes the 4e(−)/4H(+) Peractivation of O-2 to Water. *Inorg. Chem.* **2022**, *61* (14), 5442−5451.
(52) Marek, M. R. J.; Pham, T.-N.; Wang, J.; Cai, Q.; Yap, G. P. A.; Day, E. S.; Rosenthal, J. Isocorrole-Loaded Polymer Nanoparticles for Photothermal Therapy under 980 nm Light Excitation. *Acs Omega* **2022**, *7* (41), 36653−36662.
(53) Martin, M. I.; Cai, Q.; Yap, G. P. A.; Rosenthal, J. Synthesis, Redox, and Spectroscopic Properties of Pd(II) 10,10-Dimethylisocorrole Complexes Prepared via Bromination of Dimethylbiladiene Oligotetrapyrroles. *Inorg. Chem.* **2020**, *59* (24), 18241−18252.
(54) Nieto-Pescador, J.; Abraham, B.; Pistner, A. J.; Rosenthal, J.; Gundlach, L. Electronic state dependence of heterogeneous electron transfer: injection from the S-1 and S-2 state of phlorin into TiO2. *Phys. Chem. Chem. Phys.* **2015**, *17* (12), 7914−7923.
(55) Pistner, A. J.; Martin, M. I.; Yap, G. P. A.; Rosenthal, J. Synthesis, structure, electronic characterization, and halogenation of gold(III) phlorin complexes. *J. Porphyrins Phthalocyanines* **2021**, *25* (7−8), 683−695.
(56) Pistner, A. J.; Pupillo, R. C.; Yap, G. P. A.; Lutterman, D. A.; Ma, Y.-Z.; Rosenthal, J. Electrochemical, Spectroscopic, and O-1(2) Sensitization Characteristics of 10,10-Dimethylbiladiene Complexes of Zinc and Copper. *J. Phys. Chem. A* **2014**, *118* (45), 10639−10648.
(57) Potocny, A. M.; Pistner, A. J.; Yap, G. P. A.; Rosenthal, J. Electrochemical, Spectroscopic, and O-1(2) Sensitization Characteristics of Synthetically Accessible Linear Tetrapyrrole Complexes of Palladium and Platinum. *Inorg. Chem.* **2017**, *56* (21), 12703−12711.
(58) Potocny, A. M.; Riley, R. S.; O'Sullivan, R. K.; Day, E. S.; Rosenthal, J. Photochemotherapeutic Properties of a Linear Tetrapyrrole Palladium(II) Complex displaying an Exceptionally High Phototoxicity Index. *Inorg. Chem.* **2018**, *57* (17), 10608−10615.
(59) Pistner, A. J.; Lutterman, D. A.; Ghidiu, M. J.; Walker, E.; Yap, G. P. A.; Rosenthal, J. Factors Controlling the Spectroscopic Properties and Supramolecular Chemistry of an Electron Deficient 5,5-Dimethylphlorin Architecture. *J. Phys. Chem. C* **2014**, *118* (26), 14124−14132.
(60) Nelson, Z.; Delage-Laurin, L.; Swager, T. M. ABCs of Faraday Rotation in Organic Materials. *J. Am. Chem. Soc.* **2022**, *144* (27), 11912−11926.
(61) Delage-Laurin, L.; Nelson, Z.; Swager, T. M. C-Term Faraday Rotation in Metallocene Containing Thin Films. *ACS Appl. Mater. Interfaces* **2021**, *13* (21), 25137−25142.
(62) Delage-Laurin, L.; Young, H. K. S.; LaPierre, E. A.; Warndorf, M. C.; Manners, I.; Swager, T. M. C-Term Faraday Rotation in Low Symmetry tert-Butyl Substituted Polyferroceniums. *ACS macro letters* **2023**, *12*, 646−652.

https://doi.org/10.1021/acs.inorgchem.3c04004
Inorg. Chem. 2024, 63, 3630−3636